Cell Reports Medicine, Volume *5*

Supplemental information

Inhibition of CD38 enzymatic activity enhances CAR-T cell immune-therapeutic efficacy by repressing glycolytic metabolism

Yue Huang, Mi Shao, Xinyi Teng, Xiaohui Si, Longyuan Wu, Penglei Jiang, Lianxuan Liu, Bohan Cai, Xiujian Wang, Yingli Han, Youqin Feng, Kai Liu, Zhaoru Zhang, Jiazhen Cui, Mingming Zhang, Yongxian Hu, Pengxu Qian, and He Huang

Document S1. Figures S1-S10 and Table S1, related to Figure 1-7 and STAR methods.

Fig. S1 Reanalysis of single-cell level sequencing data potentiates CD38 as a hallmark of CAR-T exhaustion, related to Figure 1.

Fig. S2 CD38 inhibition reverses CART cell exhaustion through tonic signaling and reduced cytokine production in vitro independent of exhaustion model, related to Figure 2.

Fig. S3 CD38 inhibition promotes memory-like CD19-CD28z CAR-T cell formation and relieves CART cell exhaustion to improve CAR-T cytotoxicity both in vitro and in vivo, related to Figures 2 and 3.

Fig. S4 CD38 inhibition promotes memory-like GD2-CD28z CAR-T cell formation and relieves CART cell exhaustion to improve CAR-T cytotoxicity both in vitro and in vivo, related to Figures 2 and 3.

Fig. S5 CD38-knockdown phenocopies pharmacological enzymatic inhibition of CAR-T cells, related to Figures 2 and 3.

Fig. S6 Perturbing CD38 enzymatic activity reverses CAR-T cell exhaustion in bone marrow and spleen tissue as well as increases cytokine release in vivo, related to Figure 3.

Fig. S7 CD38 inhibition induces transcriptional reprogramming in CAR-T cells, related to Figure 4.

Fig. S8 78C improved CAR-T cell mitochondrial fitness while having no effect on oxidative phosphorylation, related to Figure 4.

Fig. S9 CD38 inhibition reduces CD38-cADPR-Ca^{2+} signaling, related to Figure 5.

Fig. S10 Activation of SIRT1 mimics the pharmacological CD38 enzymatic inhibition whereas CD38 monoclonal antibodies exhibit minimal impact on CAR-T cells, related to Figure 6.

Table. S1 Primer list for real-time PCR, related to STAR Methods, related to STAR Methods.

Data S1

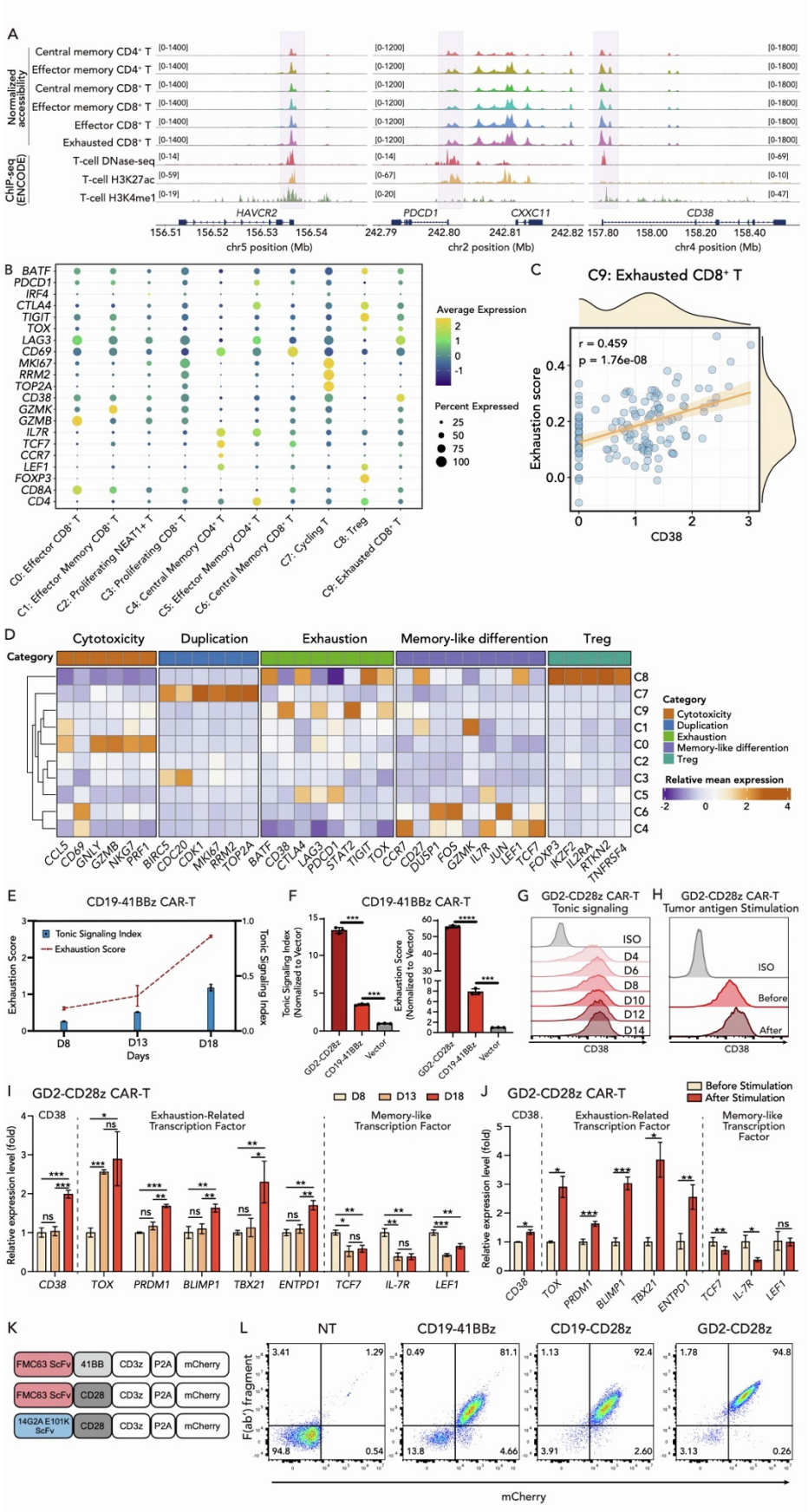
A
Normalized accessibility
Central memory CD4+ T
Effector memory CD4+ T
Central memory CD8+ T
Effector memory CD8+ T
Effector CD8+ T
Exhausted CD8+ T
ChIP-seq (ENCODE)
T-cell DNase-seq
T-cell H3K27ac
T-cell H3K4me1
HAVCR2
PDCD1
CXXC11
CD38
chr5 position (Mb)
chr2 position (Mb)
chr4 position (Mb)
B
BATF
PDCD1
IRF4
CTLA4
TIGIT
TOX
LAG3
CD69
MKI67
RRM2
TOP2A
CD38
GZMK
GZMB
IL7R
TCF7
CCR7
LEF1
FOXP3
CD8A
CD4
Average Expression
Percent Expressed
C0: Effector CD8+ T
C1: Effector Memory CD8+ T
C2: Proliferating NEAT1+ T
C3: Proliferating CD8+ T
C4: Central Memory CD4+ T
C5: Effector Memory CD4+ T
C6: Central Memory CD8+ T
C7: Cycling T
C8: Treg
C9: Exhausted CD8+ T
C
C9: Exhausted CD8+ T
r = 0.459
p = 1.76e-08
Exhaustion score
CD38
D
Cytotoxicity
Duplication
Exhaustion
Memory-like differention
Treg
Category
Relative mean expression
CCL5
CD69
GNLY
GZMB
NKG7
PRF1
BIRC5
CDC20
CDK1
MKI67
RRM2
TOP2A
BATF
CD38
CTLA4
LAG3
PDCD1
STAT2
TIGIT
TOX
CCR7
CD27
DUSP1
FOS
GZMK
IL7R
JUN
LEF1
TCF7
FOXP3
IKZF2
IL2RA
RTKN2
TNFRSF4
E
CD19-41BBz CAR-T
Tonic Signaling Index
Exhaustion Score
Exhaustion Score
Tonic Signaling Index
Days
D8
D13
D18
F
CD19-41BBz CAR-T
Tonic Signaling Index (Normalized to Vector)
Exhaustion Score (Normalized to Vector)
GD2-CD28z
CD19-41BBz
Vector
G
GD2-CD28z CAR-T
Tonic signaling
ISO
D4
D6
D8
D10
D12
D14
CD38
H
GD2-CD28z CAR-T
Tumor antigen Stimulation
ISO
Before
After
CD38
I
GD2-CD28z CAR-T
D8
D13
D18
CD38
Exhaustion-Related Transcription Factor
Memory-like Transcription Factor
Relative expression level (fold)
CD38
TOX
PRDM1
BLIMP1
TBX21
ENTPD1
TCF7
IL-7R
LEF1
J
GD2-CD28z CAR-T
Before Stimulation
After Stimulation
CD38
Exhaustion-Related Transcription Factor
Memory-like Transcription Factor
Relative expression level (fold)
CD38
TOX
PRDM1
BLIMP1
TBX21
ENTPD1
TCF7
IL-7R
LEF1
K
FMC63 ScFv
41BB
CD28
14G2A E101K ScFv
CD3z
P2A
mCherry
L
NT
CD19-41BBz
CD19-CD28z
GD2-CD28z
F(ab') fragment
mCherry
3.41
1.29
94.8
0.54
0.49
81.1
13.8
4.66
1.13
92.4
3.91
2.60
1.78
94.8
3.13
0.26

Figure S1. Reanalysis of single-cell level sequencing data potentiates CD38 as a hallmark of CAR-T exhaustion, related to Figure 1.

(A) Track plot showing chromatin accessibility and TFs binding on CD38 as well as exhaustion-associated HAVCR2 and PDCD1 loci from scATAC-seq data. DNase-seq and H3K4me1, H3K27ac ChIP-seq data were downloaded from ENCODE portal.

(B) Dot plot depicting the average expression of marker genes of each cell population from scRNA-seq data. The dot size represents the percentage of cells with values detected in each subtype. Color represents average gene activity score of each cell subtype. Dark blue means high gene expression, and light yellow means low gene expression.

(C) Correlation analysis of exhaustion score and CD38 gene expression in exhausted CD8 T cell population (Pearson's correlation test) from scRNA-seq data.

(D) Heatmap of differentially expressed genes from cytotoxicity-, duplication-, exhaustion-, memory-like differentiation-, and Treg-related gene sets in each cell population from scRNA-seq data.

(E) Exhaustion score and tonic signaling index from D8 to D18 in CD19-41BBz CAR-T cells. Red dotted line represents the exhaustion score. Blue bar represents the tonic signaling index (n=3 biological duplicates).

(F) Tonic signaling index and exhaustion score relative to empty vector in GD2-CD28z CAR-T, CD19-41BBz CAR-T and T cell transduced with empty vector, respectively, on Day 8 after retroviral transduction.

(G) Flow cytometric analysis of CD38 expression in GD2-CD28z CAR-T cells from D4 to D14 after retroviral transduction. Mean fluorescence intensity is normalized to the control at each time point.

(H) Flow cytometric analysis of CD38 expression in GD2-CD28z CAR-T cells before and after Nalm6 stimulation. Mean fluorescence intensity is normalized to the control at each time point.

(I and J) mRNA level of exhaustion-related or memory-like transcription factors in GD2-CD28z CAR-T in **I)** D8, D13 and D18 after retroviral transduction or **J)** before and after Nalm6 stimulation (n=3 biological duplicates).

(K) Schematic of three CAR constructs.

(L) Flow cytometric analysis of co-expression of mCherry and Mouse IgG, F(ab') in NT, CD19-41BBz, CD19-CD28z and GD2-CD28z CAR-T cells after sorting.

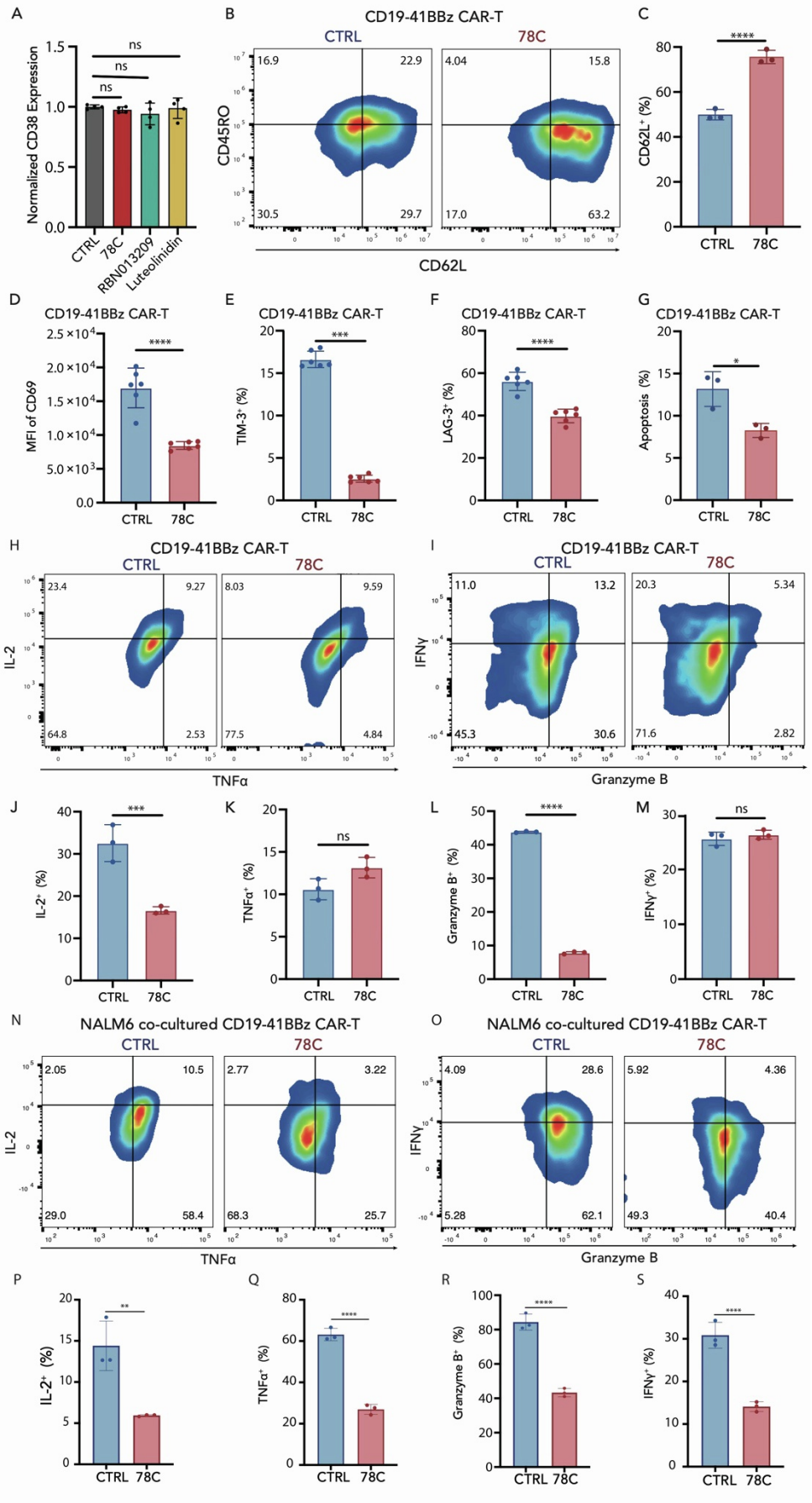
A
Normalized CD38 Expression
ns
CTRL
78C
RBN013209
Luteolinidin
B
CD19-41BBz CAR-T
CTRL
78C
CD45RO
CD62L
16.9
22.9
30.5
29.7
4.04
15.8
17.0
63.2
C
CD62L+ (%)
****
D
MFI of CD69
E
TIM-3+ (%)
***
F
LAG-3+ (%)
G
Apoptosis (%)
*
H
IL-2
TNFα
23.4
9.27
64.8
2.53
8.03
9.59
77.5
4.84
I
IFNγ
Granzyme B
11.0
13.2
45.3
30.6
20.3
5.34
71.6
2.82
J
IL-2+ (%)
K
TNFα+ (%)
ns
L
Granzyme B+ (%)
M
IFNγ+ (%)
N
NALM6 co-cultured CD19-41BBz CAR-T
2.05
10.5
29.0
58.4
2.77
3.22
68.3
25.7
O
4.09
28.6
5.28
62.1
5.92
4.36
49.3
40.4
P
IL-2+ (%)
**
Q
TNFα+ (%)
R
Granzyme B+ (%)
S
IFNγ+ (%)

Figure S2. CD38 inhibition reverses CART cell exhaustion through tonic signaling and reduced cytokine production in vitro independent of exhaustion model, related to Figure 2.

(A) Normalized CD38 expression in CAR-T cells treated with DMSO, 10uM 78C, 50uM RBN013209 or 10uM Luteolinidin for 72h on day 12 after T cell activation (n=4 biological duplicates in CTRL, 78C and RBN013209 group, n=3 biological duplicates in Luteolinidin group).

(B-C) B) Flow cytometric analysis of CD62L and CD45RO in CAR-T cells treated with DMSO or 10uM 78C for 72h on day 9 after T cell activation. C) Frequency of CD62L positive CAR-T subset in each group (n=3 biological duplicates).

(D) Frequency of CD69 positive CAR-T cells in each group. Data are mean ± SD of 6 technical duplicates from 3 donors.

(E-G) Frequency of LAG-3 positive, TIM-3 positive and PD-1 positive CAR-T cells in each group (n=6 technical duplicates from 3 different donors).

(H-M) Flow cytometric analysis of TNFα, IL-2(H), Granzyme B and IFNγ(I) and CD45RO in CAR-T cells treated with DMSO or 10uM 78C on day 12 after T cell activation. (J-M) Frequency of IL-2 positive, TNFα positive, Granzyme B positive and IFNγpositive CAR-T cells in each group (n=3 biological duplicates).

(N-S) Flow cytometric analysis of TNFα, IL-2(N) , Granzyme B and IFNγ (O) and CD45RO in CAR-T cells treated with DMSO or 10uM 78C after coculture with Nalm6 cells at 1:1 (E:T). (P-S) Frequency of IL-2 positive, TNFα positive, Granzyme B positive and IFNγpositive CAR-T cells in each group (n=3 biological duplicates).

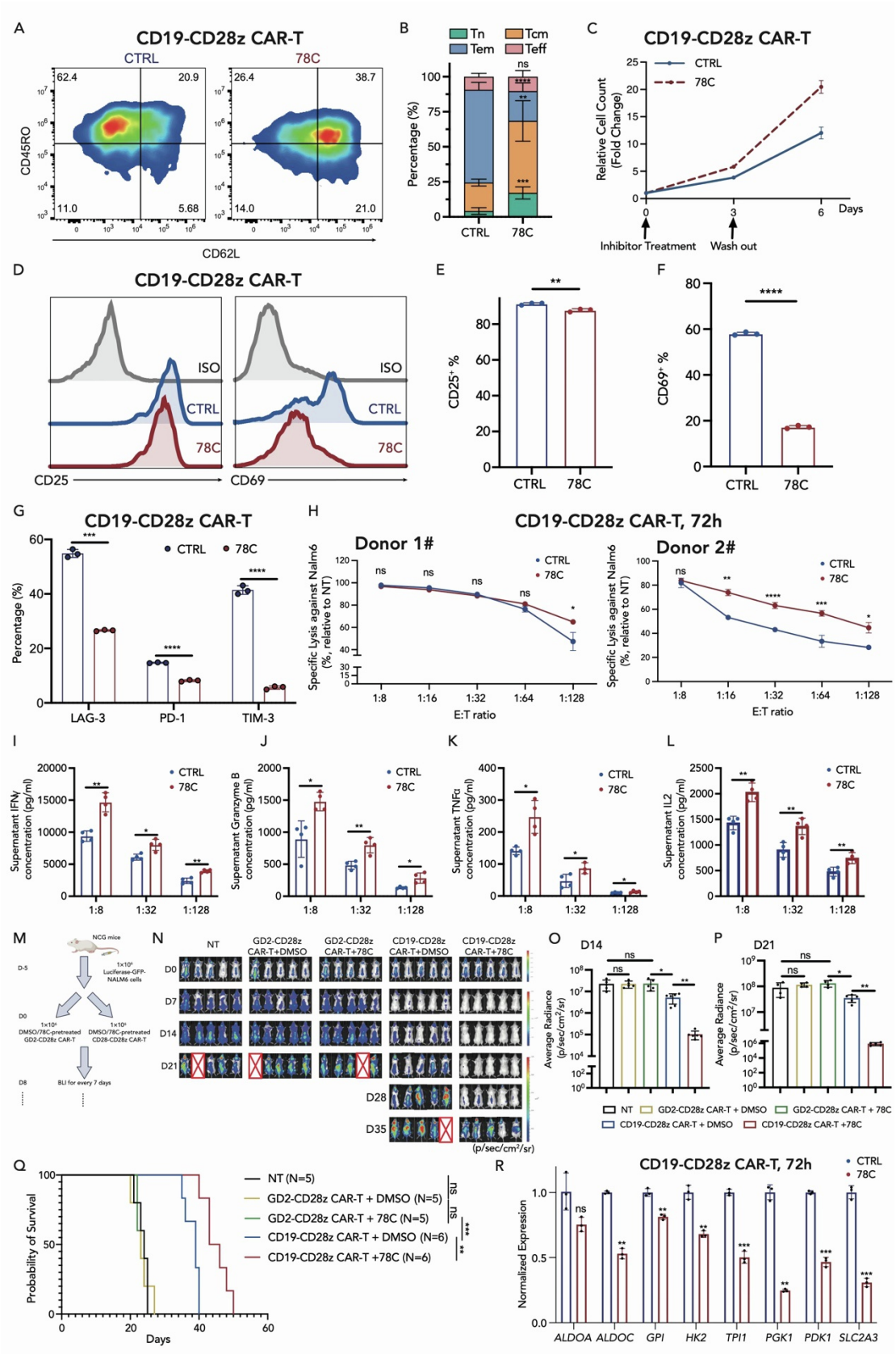

Figure S3. CD38 inhibition promotes memory-like CD19-CD28z CAR-T cell formation and

relieves CART cell exhaustion to improve CAR-T cytotoxicity both in vitro and in vivo, related to Figures 2 and 3.

(A) Flow cytometric analysis of CD62L and CD45RO in CD19-CD28z CAR-T cells treated with DMSO or 78C on day 9 after T cell activation.

(B) Frequency of Naïve cells (CD62L+, CD45RO-), central memory cells (CD62L+, CD45RO+), effector memory cells (CD62L-, CD45RO+) and effector cells (CD62L-, CD45RO-) in each group of CD19-28z CAR-T cells (n=3 biological duplicates).

(C) Expansion kinetics of control and 78C-treated CD19-CD28z CART cells during in vitro setting. Arrows indicate the time point of inhibitor treatment and drug washout (n =3 technical duplicates from one donor).

(D) Flow cytometric analysis of CD25 and CD69 expression in DMSO or 78C-pretreated CD19-CD28z CAR T cells.

(E and F) Frequency of CD25 (E) positive and CD69 (F) positive subsets in CD19-CD28z CAR-T cells treated with DMSO or 78C on day 9 after T cell activation (n=3 biological duplicates).

(G) Frequency of LAG-3 positive, TIM-3 positive and PD-1 positive subsets in CD19-CD28zCAR-T cells treated with DMSO or 78C on day 9 after T cell activation (n=3 biological duplicates).

(H) Specific lysis of Nalm6-luciferase after co-culture with control and 78C-treated CD19-CD28z CAR-T cells for 72h at low E: T ratio (n=3 technical duplicates from Donor 1 and Donor 2, respectively).

(I-L) Secretion of Granzyme B, IL-2, IFNγ and TNFα by control and 78C-treated CAR-T cells after the co-culture of Nalm6-luciferase for 72h at E: T ratio of 1:8, 1:32 and 1:128, respectively (n=4 technical duplicates).

(M) Schematic depicting in vivo experimental set-up. NSG mice received 1×10^6 Nalm6 cells on day -6 and 1×10^6 nontransduced T cells (NT), DMSO/ 78C-pretreated CD19-CD28z CAR-T cells or DMSO/78C pretreated GD2-CD28z CAR-T cells on day0. BLI imaging was done every 7 days to monitor tumor burden.

(N) D0-D35 BLI imaging of tumor clearance. n = 5 biological duplicates for each group.

(O-P) BLI imaging of tumor burden on D14 (O) and D21 (P) after CAR-T cell infusion.

(Q) Kaplan–Meyer survival plot for mice receiving NT cells (n = 5 biological duplicates), DMSO/ 78C-pretreated CD19-CD28z CAR-T cells (n = 5 biological duplicates), or DMSO/78C pretreated

GD2-CD28z CAR-T cells (n = 6 biological duplicates). Statistical analysis was performed by Mantel–Cox test between each group.

(R) mRNA level of glycolysis-related transcription factors in control or CD38-inhibited CD19-CD28z CAR T cells after coculture with Nalm6 cells (n=3 technical duplicates).

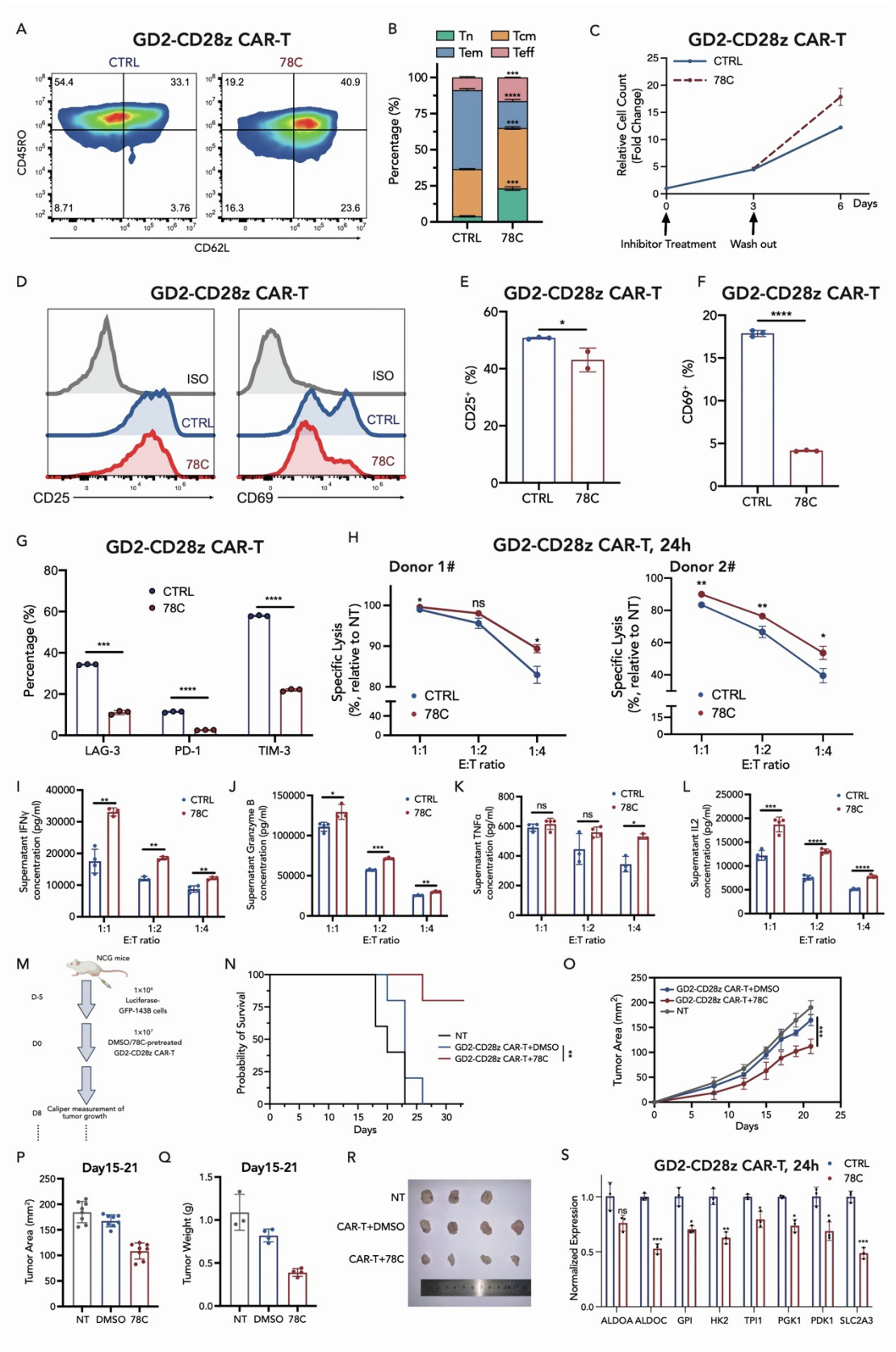

Figure S4. CD38 inhibition promotes memory-like GD2-CD28z CAR-T cell formation and relieves CART cell exhaustion to improve CAR-T cytotoxicity both in vitro and in vivo, related to

Figures 2 and 3.

(A) Flow cytometric analysis of CD62L and CD45RO in GD2-CD28z CAR-T cells treated with DMSO or 78C on day 9 after T cell activation.

(B) Frequency of Naïve cells (CD62L+, CD45RO-), central memory cells (CD62L+, CD45RO+), effector memory cells (CD62L-, CD45RO+) and effector cells (CD62L-, CD45RO-) in each group of GD2-28z CAR-T cells (n =3 biological duplicates).

(C) Expansion kinetics of control and 78C-treated GD2-CD28z CART cells during in vitro setting. Arrows indicate the time point of inhibitor treatment and drug washout (n =3 technical duplicates from one donor).

(D) Flow cytometric analysis of CD25 and CD69 expression in DMSO or 78C-pretreated GD2-CD28z CAR T cells.

(E and F) Frequency of CD25 (E) positive and CD69 (F) positive subsets in GD2-CD28z CAR-T cells treated with DMSO or 78C on day 12 after T cell activation (n =3 biological duplicates).

(G) Frequency of LAG-3 positive, TIM-3 positive and PD-1 positive subsets in GD2-CD28z CAR-T cells treated with DMSO or 78C on day 12 after T cell activation (n =3 biological duplicates).

(H) Specific lysis of 143B-luciferase after co-culture with control and 78C-treated GD2-CD28z CAR-T cells for 24h at low E: T ratio (n=3 technical duplicates from Donor 1 and Donor 2, respectively).

(I-L) Secretion of Granzyme B, IL-2, IFNγ and TNFα by control and 78C-treated CAR-T cells after the co-culture of 143B -luciferase for 24h at E: T ratio of 1:1, 1:2 and 1:4, respectively (n=4 technical duplicates).

(M) Schematic depicting in vivo experimental set-up. NSG mice received 1×10^6 143B cells via right hind leg intramuscular injection on day -6. On Day 0, 1×10^7 nontransduced T cells (NT), DMSO/78C pretreated GD2-CD28z CAR-T cells were incubated via tail vein. Tumor area was assessed every 2-5 days to monitor tumor burden.

(N) Kaplan–Meyer survival plot for mice receiving NT cells (n = 5 biological duplicates) or DMSO/78C pretreated GD2-CD28z CAR-T cells (n = 5 biological duplicates). Statistical analysis was performed by Mantel–Cox test between each group.

(O) Analysis of tumor clearance. Data are mean ± SD of n = 5 mice in each group. Two-way analysis of variance (ANOVA) test with Dunnett's multiple comparison test. ***$P < 0.001$.

(P) Caliper measurement of tumor growth D15-21 after CAR-T cell infusion. Data are mean ± SD of n

= 7 biological duplicates pooled by two independent experiments.

(Q and R) Q) Tumor weight on Day 15-21 after CAR-T cell infusion for mice receiving NT cells (n = 3 biological duplicates) or DMSO/78C pretreated GD2-CD28z CAR-T cells (n = 4 biological duplicates). When mice in NT group reach follow-up endpoint, mice in each group were sacrificed for tumor removal. R) 143B tumor analysis on Day 15-21 after CAR-T cell infusion in each group.

(S) mRNA level of glycolysis-related transcription factors in control or CD38-inhibited GD2-CD28z CAR T cells after coculture with Nalm6 cells (n=3 technical duplicates).

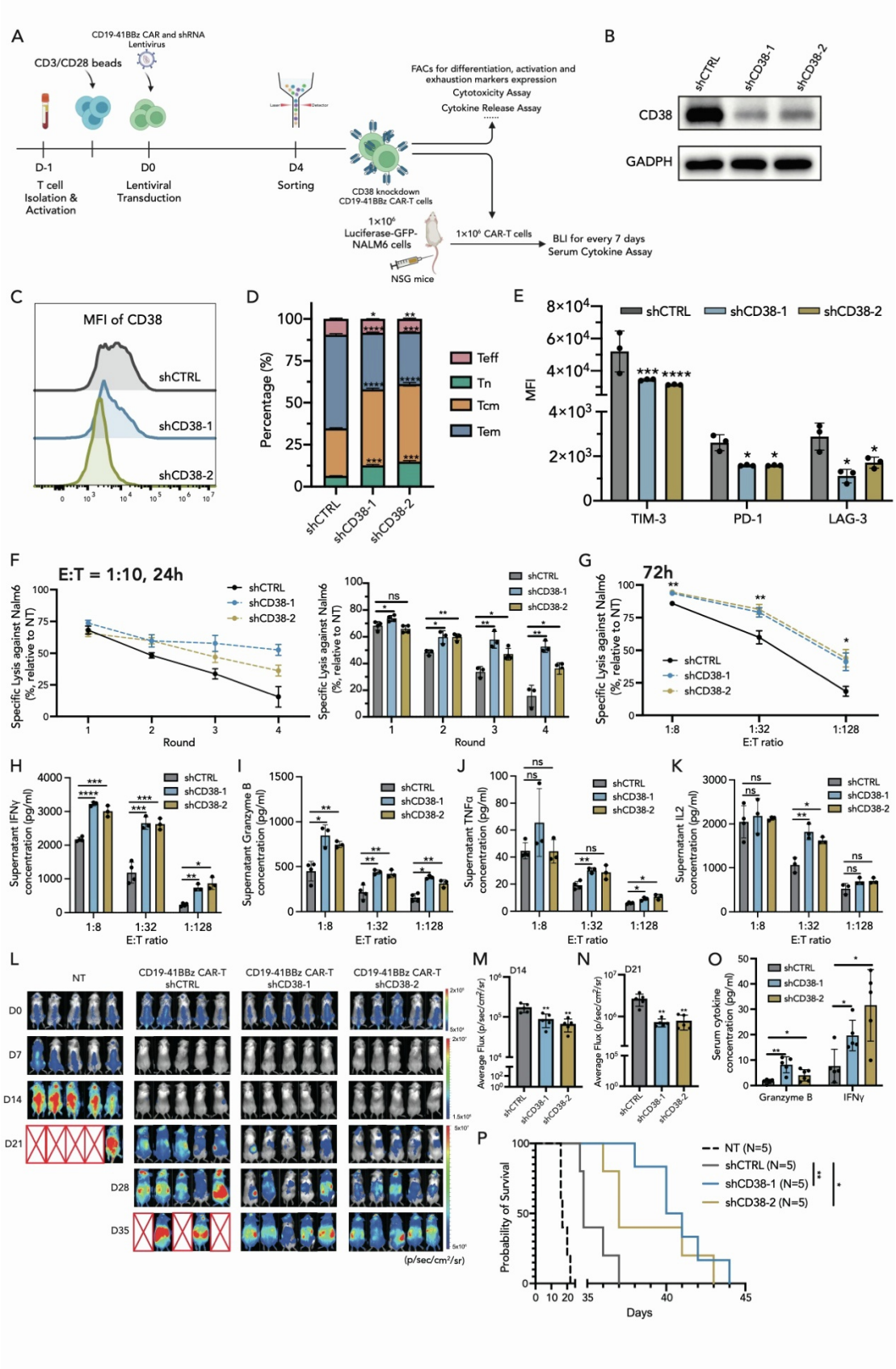

Figure S5. CD38-knockdown phenocopies pharmacological enzymatic inhibition of CAR-T cells,

related to Figures 2 and 3.

(A) Schematic depicting in vitro and in vivo experiments of CD38-knockdown CD19-41BBz CAR-T cells. CD19-41BBz CAR and shRNA lentivirus were transduced on Day 0. After sorting on Day 4, CAR-T cells were cultured until Day 12 for flow cytometric analysis, cytotoxicity assay and cytokine release assay in vitro. For the in vivo experiment, NSG mice were injected intravenously with 1.0×10^6 Nalm6 leukemia and treated with 1.0×10^6 nontransduced T and scramble- or CD38-knockdown CD19-41BBz CAR T cells 6 days after tumor infusion (n = 5 biological duplicates).

(B) Western Blot analysis of CD38 in shCTRL, shCD38-1, shCD38-2 CD19-41BBz CAR-T cells. Quantitative analysis of western blot data obtained in n = 3 experiments is shown, normalized to GAPDH.

(C) Flow cytometric analysis of CD38 expression in shCD38-1, shCD38-2 and shCTRL CAR-T cells.

(D) Frequency of Naïve cells (CD62L+, CD45RO-), central memory cells (CD62L+, CD45RO+), effector memory cells (CD62L-, CD45RO+) and effector cells (CD62L-, CD45RO-) in each group (n=3 donors). Statistical comparison is between the control and each CD38-knockdown CAR-T group.

(E) Frequency of LAG-3 positive, TIM-3 positive and PD-1 positive subsets in shCD38-1, shCD38-2 and shCTRL CAR-T cells (n=3 biological duplicates). Statistical comparison is between the control and each CD38-knockdown CAR-T group.

(F) Specific lysis of Nalm6-luciferase after co-culture with control and CD38-knockdown CD19-41BBz CAR-T cells upon multiple rounds of tumor challenge at the E: T = 1:10 for every 24h (n=3 technical duplicates). Statistical comparison is between the control and each CD38-knockdown CAR-T group.

(G) Specific lysis of Nalm6-luciferase after co-culture with control and 78C-treated CAR-T cells for 72h at low E: T ratio (n=3 technical duplicates). Statistical comparison is between the control and each CD38-knockdown CAR-T group.

(H-K) Secretion of Granzyme B, IL-2, IFNγ and TNFα by control and 78C-treated CAR-T cells after the co-culture of Nalm6-luciferase for 72h at E:T ratio of 1:1 and 1:128, respectively (n=3 technical duplicates).

(L) D0-D35 BLI imaging of tumor clearance. n = 5 biological duplicates for each group.

(M and N) BLI imaging of tumor burden on D14 (M) and D21 (N) after CAR-T cell infusion.

(O) Serum concentration of Granzyme B and IFNγ in control or CD38-knockdown groups on day 8

after CD19-41BBz CAR-T infusion (n =5 biological duplicates in each group).

(P) Kaplan–Meyer survival plot for mice receiving NT cells shCTRL, shCD38-1 or shCD38-2 CD19-41BBz CAR-T cells (n = 5 biological duplicates in each group). Statistical analysis was performed by Mantel–Cox test between control and each CD38-knockdown CAR-T group.

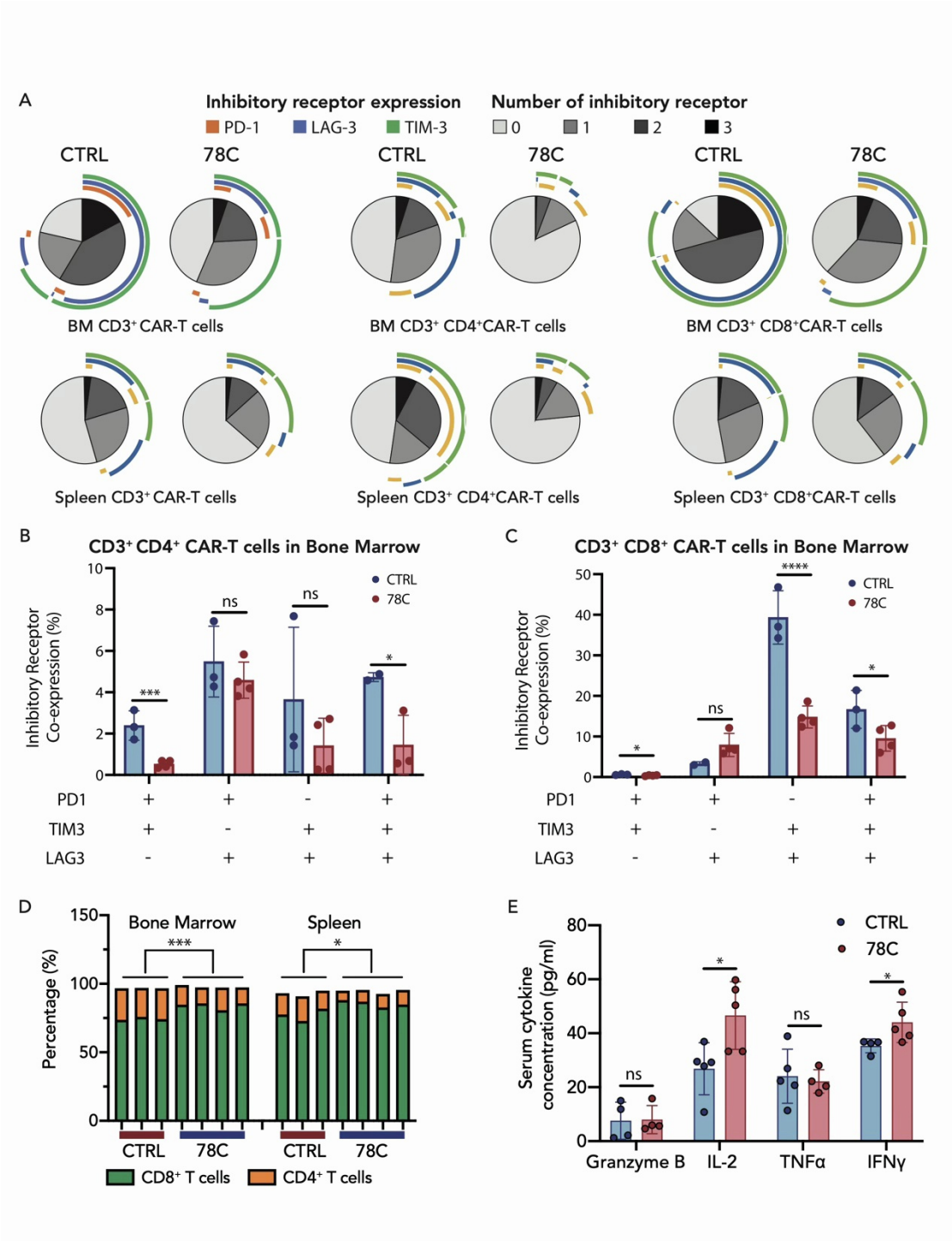

Figure S6. Perturbing CD38 enzymatic activity reverses CAR-T cell exhaustion in bone marrow and spleen tissue as well as increases cytokine release in vivo, related to Figure 3.

(A) Patterns of expression and co-expression of the inhibitory molecules PD-1, TIM-3, and LAG-3 in CD4 or CD8 T cells in BM and Spleen. The numbers of positive-expression of inhibitory receptors: none (PD1-TIM3-LAG3-), one (PD1+TIM3-LAG3- or PD1-TIM3+LAG3- or PD1-TIM3-LAG3+), two (PD1+TIM3+LAG3- or PD1+TIM3-LAG3+ or PD1-TIM3+LAG3+), and three

(PD1+TIM3+LAG3+) are depicted, which were detected by FACS. BM: bone marrow

(B and C) Frequency of inhibitory receptor co-expression (LAG-3, TIM-3 and PD-1) of CD4 positive (B) or CD8 positive (C) CAR-T cells from bone marrow in control or 78C-pretreated groups on day 8 after CAR-T infusion (n=3 biological duplicates in the control group, n=4 biological duplicates in 78C-pretreated groups).

(D) Frequency of CD4 positive and CD8+ positive T cells in vivo in control or 78C-pretreated groups from bone marrow and spleen on day 8 after CAR-T infusion (n=3 biological duplicates in the control group, n=4 biological duplicates in 78C-pretreated groups).

(E) Serum concentration of Granzyme B, IL-2, TNFαand IFNγ in control or 78C-pretreated groups on day 8 after CAR-T infusion (n=3 or more biological duplicates in each group).

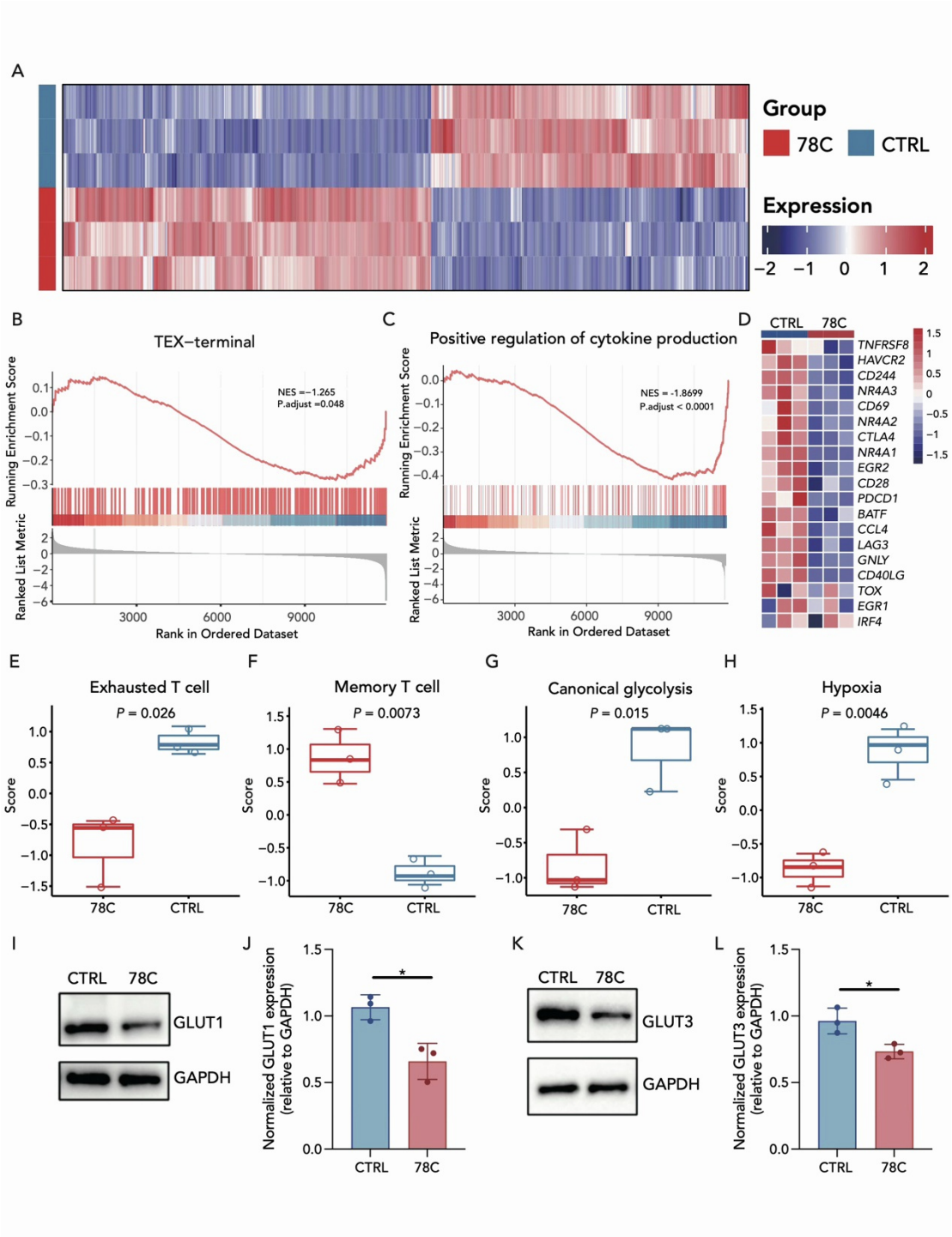

Figure S7. CD38 inhibition induces transcriptional reprograming in CAR-T cells, related to Figure 4.

(A) Heatmap showing the FPKM values of a total of 749 DEGs in comparisons with the control group.

(B) Enrichment plot of the terminal exhausted T cell from the gene set identified in the LCMV mouse model (PMID: 32396847)

(C) Enrichment plot of the positive regulation of cytokine production from the GO gene set obtained

performing GSEA.

(D) Heatmap of differential expressed T cell exhaustion-related genes in comparisons with the control group.

(E-H) Bar plot of selected pathways enriched in genes significantly upregulated or downregulated in 78C-treated CAR-T cells according to Gene Set Variation Analysis results. For each pathway, a single sample enrichment score was calculated, and the mean was taken per response group. The mean normalized enrichment score (ranging from –2 to +2) of pathways enriched in induced (red) or repressed (blue) genes was presented.

(I and J) Western blot analysis of GLUT1, Nalm6 stimulated CD19-41BBz CAR-T cells were treated with DMSO/78C for 3 days. Quantitative analysis of western blot data obtained in n = 3 biological duplicates is shown, normalized to GAPDH.

(K and L) Western blot analysis of GLUT3, Nalm6 stimulated CD19-41BBz CAR-T cells were treated with DMSO/78C for 3 days. Quantitative analysis of western blot data obtained in n = 3 biological duplicates is shown, normalized to GAPDH.

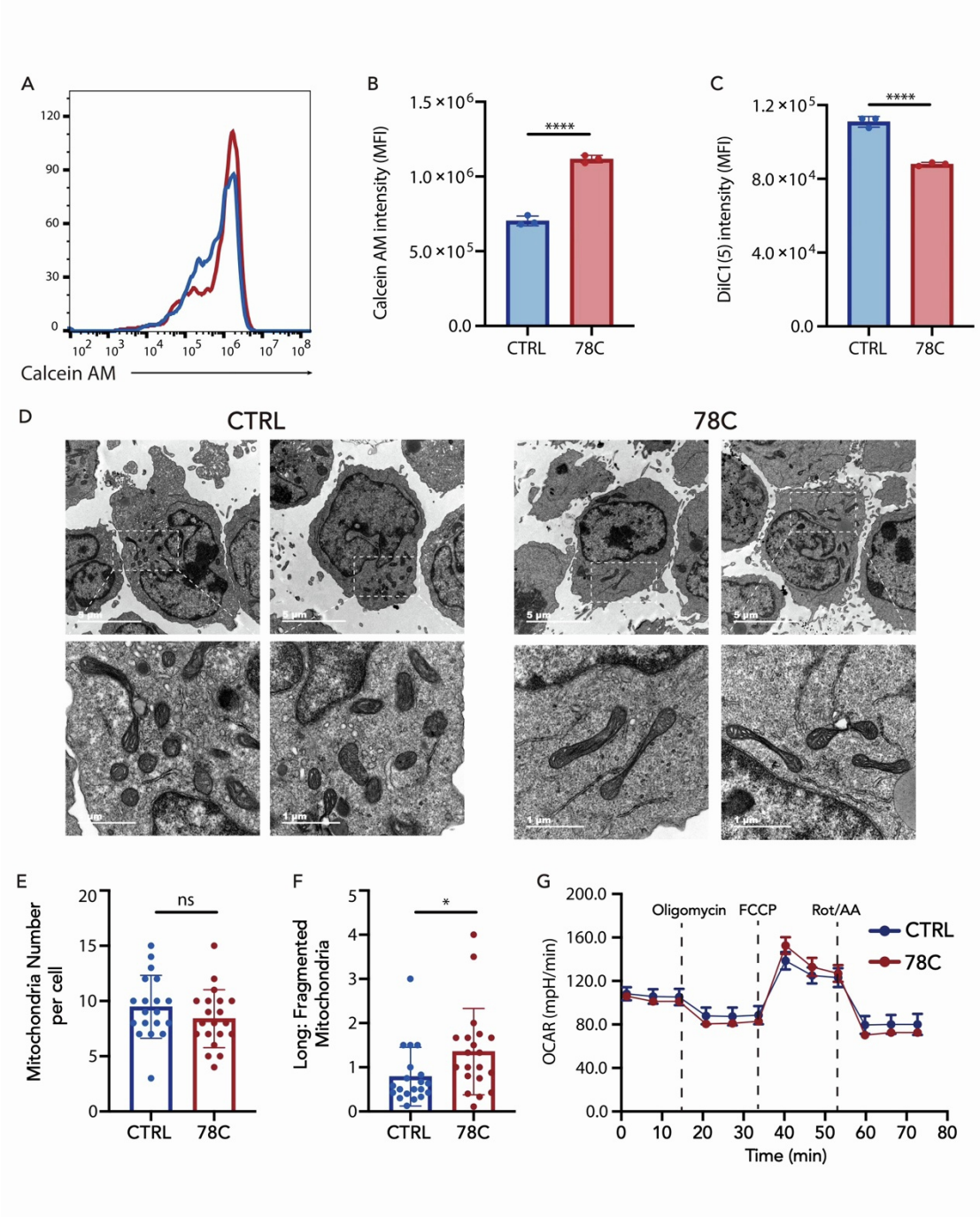

Fig. S8 78C improved CAR-T cell mitochondrial fitness while has no effect on oxidative phosphorylation, related to Figure 4.

(A and B) (A) Flow cytometry analysis showing calcein fluorescence treated with calcein-AM (1 μM) and Co2+ (1 mM) under basal conditions in control or 78C-treated CAR-T cells. (B) Median Fluorescence Intensity of calcein-AM after FACS analysis in control or 78C-treated CAR-T (n=3 biological duplicates).

(C) Median Fluorescence Intensity of DiIC1(5) indicating mitochondrial membrane potential in control

or 78C-treated CAR-T (n=3 biological duplicates.

(D) Representative transmission electron microscopic images of mitochondrial morphology in control CART and CD38-inhibited CART cells 12 days after T cell activation

(E and F) Bar graph illustrating quantitation of mitochondria number per cell (E) and the ratio of mitochondria fusion to mitochondria fission. (n = 20 independent fields). Scale bars, 500 nm.

(G) Metabolic rate as measured by Seahorse analysis of oxygen consumption rate (OCR) of control or CD38-inhibited CAR T cells after coculture with Nalm6 cells (n=5 technical duplicates).

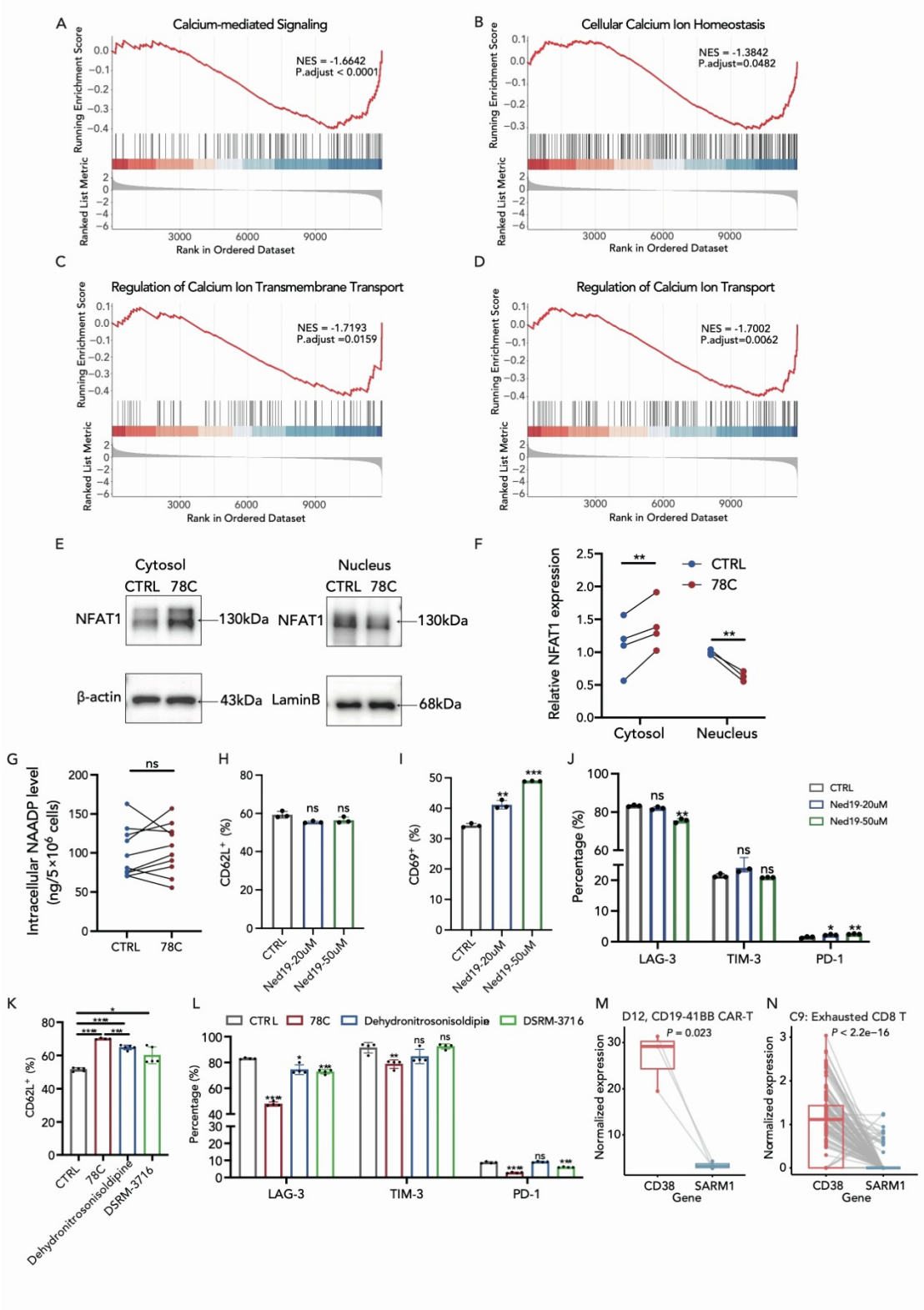

Figure S9. CD38 inhibition reduces CD38-cADPR-Ca2+ signaling, related to Figure 5.

(A-D) Enrichment plot of the calcium-mediated signaling (A), cellular calcium homeostasis (B), regulation of calcium ion transmembrane transport (C) and regulation of calcium ion transport (D) from the GO gene set.

(E and F) Western blot analysis of NFAT1, Nalm6 stimulated CAR-T cells were treated with DMSO/78C for 3 days and the cytoplasmic proteins and nuclear proteins were separated. Quantitative analysis of western blot data obtained in n = 4 experiments is shown, normalized to β-Actin or Lamin B.

(G) Intracellular NAADP level in control or 78C-treated CAR-T cells after coculture with Nalm6 cells (n=8, 4 biological replicates with 2 technical replicates for each donor).

(H) Frequency of CD62L positive CAR-T subset in CD19-41BBz CAR-T cells treated with DMSO or NAADP inhibitor, Ned19 (n=3 biological replicates).

(I) Frequency of CD69 positive CAR-T cells in CD19-41BBz CAR-T cells treated with DMSO or NAADP inhibitor, Ned19 (n=3 biological replicates).

(J) Frequency of LAG-3 positive, TIM-3 positive and PD-1 positive subsets in CD19-41BBz CAR-T cells treated with DMSO or NAADP inhibitor, Ned19 (n=3 biological replicates).

(K) Frequency of CD62L positive CAR-T subset in CD19-41BBz CAR-T cells treated with DMSO, 78C or SARM1 inhibitor, Dehydronitrosonisoldipine and DSRM-3716 (n=5 biological replicates).

(L) Frequency of LAG-3 positive, TIM-3 positive and PD-1 positive subsets in CD19-41BBz CAR-T cells treated with DMSO, 78C or SARM1 inhibitor, Dehydronitrosonisoldipine and DSRM-3716 (n=4 biological replicates).

(M) Normalized expression of CD38 and SARM1 in bulk RNA-seq data of CD19-41BBz CAR-T cells on Day 12.

(N) Normalized expression of CD38 and SARM1 in C9 cluster from scRNA-seq dataset. Statistical analysis was performed by two-tailed, paired T test of normalized expression within each single cell.

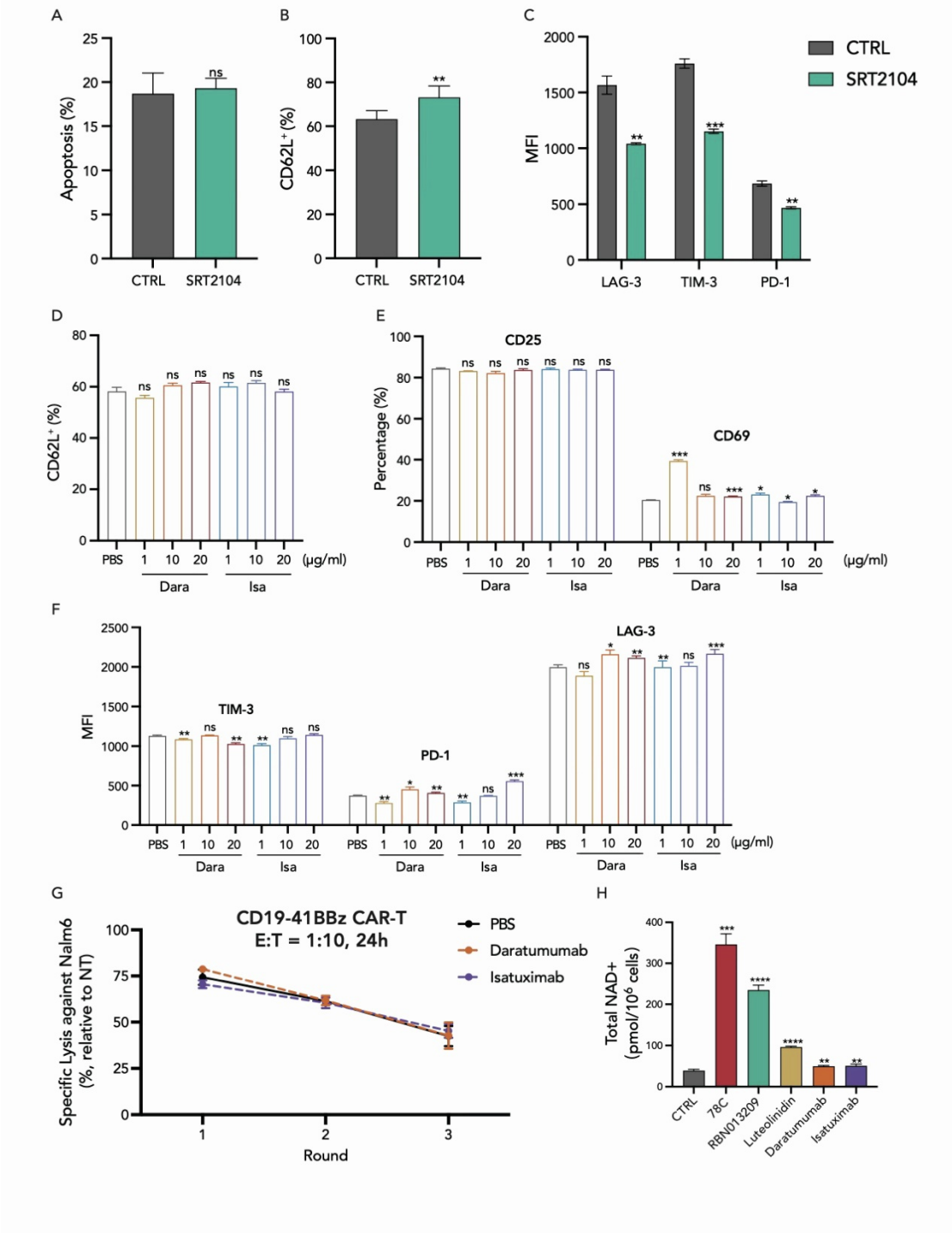

Figure S10. Activation of SIRT1 mimics the pharmacological CD38 enzymatic inhibition whereas CD38 monoclonal antibodies exhibit minimal impact on CAR-T cells, related to Figure 6.

(A) Frequency of apoptosis (Annexin V positive) in CD19-41BBz CAR-T cells treated with DMSO or SIRT1 activator, SRT2104 (n=3 biological duplicates).

(B) Frequency of CD62L positive CAR-T subset in CD19-41BBz CAR-T cells treated with DMSO or SIRT1 activator, SRT2104 (n=3 biological replicates).

(C) Frequency of LAG-3 positive, TIM-3 positive and PD-1 positive subsets in CD19-41BBz CAR-T cells treated with DMSO or SIRT1 activator, SRT2104 (n=3 biological replicates).

(D) Frequency of CD62L positive CAR-T subset in CD19-41BBz CAR-T cells treated with PBS, Daratumumab or Isatuximab (n=3 biological replicates). Statistical analysis was performed between each experimental group with PBS group.

(E) Frequency of CD25 and CD69 positive CAR-T subsets in CD19-41BBz CAR-T cells treated with PBS, Daratumumab or Isatuximab (n=3 biological replicates). Statistical analysis was performed between each experimental group with PBS group.

(F) Frequency of LAG-3 positive, TIM-3 positive and PD-1 positive subsets in CD19-41BBz CAR-T cells treated with PBS, Daratumumab or Isatuximab (n=3 biological replicates). Statistical analysis was performed between each experimental group with PBS group.

(G) Specific lysis of Nalm6-luciferase after co-culture with control and CD38 antibodies-treated CD19-41BBz CAR-T cells upon multiple rounds of tumor challenge at the E: T=1:10 for every 24h (n=3 technical replicates). Statistical comparison is between each experimental group with PBS group.

(H) Total NAD+ level CD19-41BBz CAR-T cells treated with PBS, 78C, RBN013209, Luteolinidin, Daratumumab or Isatuximab after coculture with Nalm6 cells (n=4, 2 biological replicates with 2 technical replicates for each donor). Statistical comparison is between each experimental group with PBS group.

Table. S1 Primer list for real-time PCR, related to STAR Methods.

Gene	Primer	Sequence (5'-3')
CD38	F	GCGATGCGTCAAGTACAC
	R	GTACGGTCTGAGTTCCCAA
TBX21	F	GGAAGTGGGGCTCAAGAA
	R	AAACCAAAAGCAAGACGCA
TOX	F	AGCAACTCGCAGCATACA
	R	CATGGCAGTTAGGTGAGGA
PRDM1	F	AAGCAACTGGATGCGCTATGT
	R	GGGATGGGCTTAATGGTGTAGAA
TCF7	F	CTGGCTTCTACTCCCTGACCT
	R	ACCAGAACCTAGCATCAAGGA
IL-7R	F	CCCTCGTGGAGGTAAAGTGC
	R	CCTTCCCGATAGACGACACTC
NRF2	F	CACATCCAGTCAGAAACCAGTGG
	R	GGAATGTCTGCGCCAAAAGCTG
PRDM1	F	AAGCAACTGGATGCGCTATGT
	R	GGGATGGGCTTAATGGTGTAGAA
PDCD1	F	CCAGGATGGTTCTTAGACTCCC
	R	TTTAGCACGAAGCTCTCCGAT
RUNX1	F	CTGCCCATCGCTTTCAAGGT
	R	GCCGAGTAGTTTTCATCATTGCC
CTLA4	F	GAACACCGCTCCCATAAA
	R	TTTGCAGAAGACAGGGATG
FOS	F	CCGGGGATAGCCTCTCTTACT
	R	CCAGGTCCGTGCAGAAGTC
ENO2	F	AGCCTCTACGGGCATCTATGA
	R	TTCTCAGTCCCATCCAACTCC
FOXK1	F	TCCAGGAGCCGCACTTCTA

	R	CTCCGGGATGTGGATCTTCA
ALDOA	F	ATGCCCTACCAATATCCAGCA
	R	GCTCCCAGTGGACTCATCTG
ALDOC	F	ATGCCTCACTCGTACCCAG
	R	TTTCCACCCCAATTTGGCTCA
GPI	F	CAAGGACCGCTTCAACCACTT
	R	CCAGGATGGGTGTGTTTGACC
HK2	F	AGCCCTTTCTCCATCTCCTT
	R	AACCATGACCAAGTGCAGAA
PFKM	F	GGTGCCCGTGTCTTCTTTGT
	R	AAGCATCATCGAAACGCTCTC
PKM	F	GTGCAGAAGAGAGCGATCCG
	R	CGGTTAGACCCCCATAGTGC
PGAM	F	ATGTCGAAGCCCCATAGTGAA
	R	TGGGTGGTGAATCAATGTCCA
TPI1	F	CTCATCGGCACTCTGAACG
	R	GCGAAGTCGATATAGGCAGTAGG
Pgk1	F	TGGACGTTAAAGGGAAGCGG
	R	GCTCATAAGGACTACCGACTTGG
PDK1	F	CTGTGATACGGATCAGAAACCG
	R	TCCACCAAACAATAAAGAGTGCT
SGK1	F	AGGATGGGTCTGAACGACTTT
	R	GCCCTTTCCGATCACTTTCAAG
SLC2A3	F	GCTGGGCATCGTTGTTGGA
	R	GCACTTTGTAGGATAGCAGGAAG
Myc	F	GGCTCCTGGCAAAAGGTCA
	R	CTGCGTAGTTGTGCTGATGT
Eno1	F	AAAGCTGGTGCCGTTGAGAA
	R	GGTTGTGGTAAACCTCTGCTC

ACTB	F	CATGTACGTTGCTATCCAGGC
	R	CTCCTTAATGTCACGCACGAT